 doi:10.20944/preprints202105.0672.v1

Unveiling the Ionic Diels-Alder Reactions within the Molecular Electron Density Theory

Luis R. Domingo,[1*] Mar Ríos-Gutiérrez[1] and María José Aurell[1]

[1]*Department of Organic Chemistry, University of Valencia, Dr. Moliner 50, E-46100 Burjassot, Valencia, Spain,*

E-mail: domingo@utopia.uv.es

Abstract

The ionic Diels-Alder (I-DA) reactions of a series of six iminium cations with cyclopentadiene have been studied within the Molecular Electron Density Theory (MEDT). The superelectrophilic character of iminium cations, $\omega > 8.20$ eV, accounts for the high reactivity of these species participating in I-DA reactions. The activation energies are found between 13 and 20 kcal·mol^{-1} lower in energy than those associated to the corresponding Diels-Alder (DA) reactions of neutral imines. These reactions are low *endo* selective as a consequence of the cationic character of the TSs, but highly regioselective. Solvents have poor effects on the relative energies, and an unappreciable effect in the geometries. In dichloromethane the activation energies increase slightly as a consequence of the better solvation of the iminium cations than the cationic TSs. ELF topological analysis of the bonding changes along the I-DA reactions shows that they are very similar to those in polar DA reactions. The present MEDT study makes it possible establishing that the global electron density transfer (GEDT) taking place at the TSs of I-DA reactions, and not steric (Pauli) repulsions such as have been recently proposed, are responsible for the features of these type of DA reactions.

Keywords: ionic Diels-Alder reactions, Molecular Electron Density Theory, iminium cations, superelectrophiles, global electron density transfer, asynchronicity.

Preprints (www.preprints.org) | NOT PEER-REVIEWED | Posted: 27 May 2021 doi:10.20944/preprints202105.0672.v1

1. Introduction.

The Diels-Alder (DA) reaction between a conjugated diene and an ethylene to yield a cyclohexene, reported for the first time by Diels and Alder in 1928 [1], is one of the most studied organic reactions from a synthetic as well as a theoretical viewpoint (see Scheme 1) [2,3].

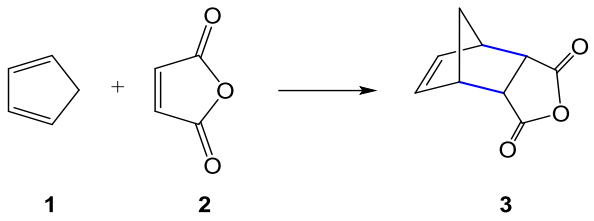

Scheme 1. DA reaction between Cp **1** and maleic anhydride **2** reported in 1928 by Diels and Alder.

The mechanism of the DA reaction has been the subject of an amount of theoretical studies. The most accepted one is the "pericyclic mechanism" proposed by Woodward and Hoffman in 1969 [4], and further supported by Houk in 1995 [5]. The "pericyclic mechanism" concept refers as the electron density changes along the DA reactions, but this mechanism never was quantum chemically proved until 2002 in which a Bonding Evolution Theory [6] (BET) study of the DA reaction between butadiene **4** and ethylene **5** showed that the changes on electron density take place sequentially along a symmetry plane (see Scheme 2) [7,8].

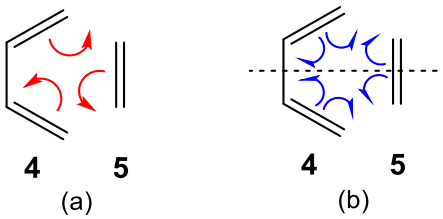

Scheme 2. Changes in electron density in the DA reaction between butadiene **4** and ethylene **5**: (a) those proposed in the pericyclic mechanism [4]; (b) those resulting of a BET analysis [8].

After an exhaustive study of organic reactions carried out along 20 years, in 2016 Domingo proposed the Molecular Electron Density Theory [9] (MEDT) for the study of the organic reactivity. MEDT, which goes against any reactivity model based on the analysis of molecule orbitals (MOs) such as proposed the Frontier Molecular Orbital (FMO) theory [10], allowed recently to reject both the "pericyclic mechanism" [8]

Preprints (www.preprints.org) | NOT PEER-REVIEWED | Posted: 27 May 2021 doi:10.20944/preprints202105.0672.v1

proposed by Woodward and Hoffman and the "aromatic transition state structures (TSs)" proposed by Dewar [11].

An exhaustive theoretical study on experimental DA reactions, allowed establishing the definitive role of the global electron density transfer [12] (GEDT) taking place at the TSs in the feasibility of DA reactions [13,14]. This finding allowed establishing in 2009 the mechanism of the polar DA (P-DA) reactions [15], in which the favourable nucleophilic/electrophilic interactions taking place at the TSs is responsible for the feasibility of the reaction. The very good correlation found between the GEDT and the activation barriers for the DA reactions of Cp **1** with a series of 12 substituted ethylenes, including iminium cation **6**, allowed the classification of the DA reactions in non-polar DA (N-DA), which do not take place easily experimentally, P-DA reactions, and ionic DA (I-DA) reaction, in which one of the two reagents is an ionic species (see Figure 1) [15]. In this sent, the analysis of the electrophilicity [16] ω and nucleophilicity [17] *N* indices defined within the Conceptual DFT [18,19] (CDFT) has becomes a powerful tool for experimentalist organic chemists to study easily DA reactions [15].

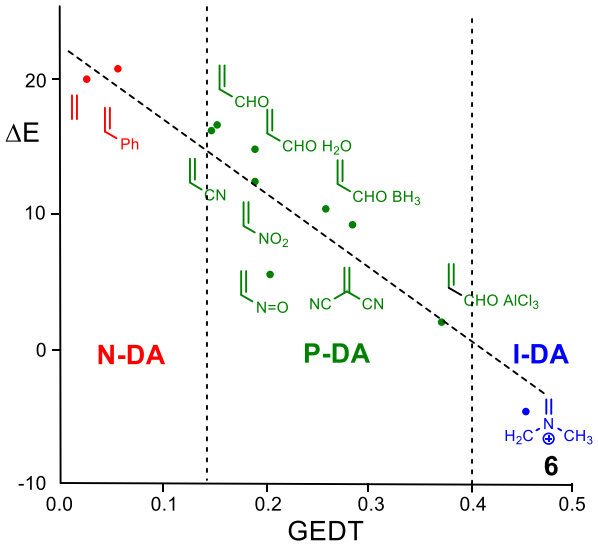

Figure 1. Plot of the activation barriers (ΔE in kcal·mol^{-1})) *vs.* the GEDT, e, R^2 = 0.89, for the DA reactions of Cp **1** with the substituted ethylene series of an increased electrophilic character. The classification of the DA reactions, based on the GEDT, is included.

Iminium cation **6** was found the most reactive species, showing the highest electrophilicity ω index, 8.24 eV. This very high value, which classifies it as a superelectrophile [20,21], is a consequence of its cationic nature. Although, I-DA reactions can be understood as the extreme of P-DA reactions, the different behaviours

Preprints (www.preprints.org) | NOT PEER-REVIEWED | Posted: 27 May 2021 doi:10.20944/preprints202105.0672.v1

of the TSs involved in I-DA reactions with respect to those of P-DA reactions, demanded its classification as I-DA reactions (see Figure 1)[15].

Although, many I-DA reactions have been described in the literature, the majority of them involves cationic species such as cationic derivatives of imines. This behaviour is a consequence of the fact that while superelectrophilic species react with poor or marginal nucleophiles, supernucleophilic species, such as anionic species, do no react effectively with poor or marginal electrophiles. Thus, Sauer et al. studied the DA reactions between several salts of iminium cation **6** and substituted butadienes **7**, both experimentally and theoretically using AM1 semiempirical calculations (see Scheme 3) [22]. These authors suggested that the DA reactions of iminium cation **6** with the acyclic 1,3-butadienes **7** proceeded via transition state structures (TSs) that closely resemble to those yielding intermediate allyl cations. Only in the case of reaction with Cp **1** these authors concluded that the reaction takes place along a pericyclic TS [22].

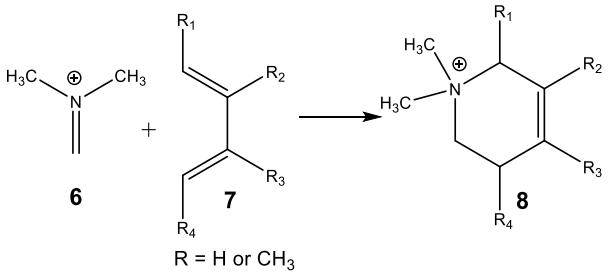

Scheme 3. I-DA reactions experimental and theoretically studied by Sauer et al. [22].

Andersson et al. explored the DA reaction between Cp **1** and a family of chiral imines containing a second nitrogen atom at a conjugated position, because in a strong acid medium the protonation of this nitrogen atom might fulfil the role of an electron-withdrawing group [23]. Thus, when imine **9** was treated with Cp **1** under strong acid conditions a –78 ºC, a highly stereoselective cycloaddition took place giving the pyridine-substituted aza-norbornene **10** in good yield (see Scheme 4). Note that this reaction is a Bronsted acid catalysed DA reaction of the imine **9**.

.

Preprints (www.preprints.org) | NOT PEER-REVIEWED | Posted: 27 May 2021 doi:10.20944/preprints202105.0672.v1

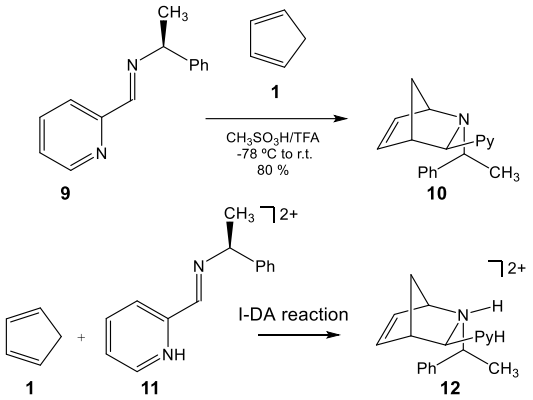

Scheme 4. I-DA reactions experimentally studied by Andersson et al. [23].

The participation of cationic species as the heterodiene or the ethylene derivative in DA reactions have been widely studied in the literature. Thus, in 2001 the I-DA reaction between iminium cation **6** and Cp **1**, experimentally studied by Sauer [22], was studied at the B3LYP/6-31G(d) and MP2/6-31G(d)levels [24]. This study allowed to conclude that this I-DA reaction takes place via a one-step mechanism involving a highly asynchronous TS with a high GEDT. A complete analysis of the features of the TS indicated that this I-DA reaction can be characterized by the nucleophilic attack of Cp **1** on the carbon of the electron-poor iminium cation **6** instead of a "pericyclic process". The concomitant ring closure affords the final cycloadduct without the participation of any allyl cation intermediate, via a non-concerted *two-stage one-step* mechanism [25]. In consequence, iminium cation **6** and Cp **1** behave as electrophile and nucleophile, respectively, instead of as dienophile and diene.

The I-DA reaction of Cp **1** with diprotonated imine **11**, experimentally reported by Andersson [23], was theoretically studied using HF/6-31G* and B3LYP/6-31G methods [26]. This I-DA reaction takes place along a two-step mechanism. The first step corresponds to the nucleophilic attack of Cp **1** on the carbon of the iminium cation group to give an acyclic cation intermediate, while the second step is associated with the ring closure of this intermediate along the formation of the second C–N single bond yielding the final cycloadduct **12**. Protonation of both pyridine and imine nitrogen atoms increases strongly the electrophilicity of the imine, and the I-DA reaction takes place along a favourable inverted energy profile, allowing the justification of the large acceleration of the reaction in a strong acid medium [23]. The inclusion of solvent effects yielded a negligible variation of the energy profile.

In 2014, Domingo performed a quantum chemical topological analysis of the C–C bond formation in organic reactions involving cationic species [27]. To this end, the I-

 doi:10.20944/preprints202105.0672.v1

DA reaction between the iminium cation **6** and Cp **1** was chosen as computational model. The BET analysis showed that C–C bond formation begins at the C-C distance of 1.96 Å via a C-to-C *pseudoradical* coupling between the most electrophilic center of the iminium cation and one of the two most nucleophilic centers of Cp. Interestingly, this pattern for the formation of the C–C single bond was identical to that found in the N-DA reaction between butadiene **4** and ethylene **5** [12]. Analysis of the Parr functions [28] allowed characterising the most electrophilic and nucleophilic center of the reagents participating in this I-DA reaction.

Very recently, Bickelhaup et al. studied using an energy decomposition analysis the origin of rate enhancement and asynchronicity in iminium catalyzed DA reactions [29]. Through their activation strain [30] and Kohn–Sham molecular orbital [31] analyses these authors suggested that "the iminium catalysts enhance the reactivity by reducing the steric (Pauli) repulsion between the diene and dienophile, which originates from both a more asynchronous reaction mode and a more significant polarization of the π-system away from the incoming diene compared to aldehyde and imine analogs". They concluded that "the driving force behind the asynchronicity of these DA reactions is the relief of destabilizing steric (Pauli) repulsion and not the orbital interaction between the terminal carbon of the dienophile and the diene" [29].

The asynchronicity in cycloaddition reactions have been widely studied within the polar reaction model [13-15]. P-DA reactions involving symmetric electrophilic ethylenes such as anhydride maleic or tetracyanoethylene take place trough synchronous TSs [14], while the use of non-symmetric electrophilic ethylenes such as nitroethylene or 1,1-dicyanoethylene yields highly asynchronous TSs [13-15,32] These studies emphasised that along an asynchronous single bond formation process, the more favourable two-center interaction begins at the most electrophilic and nucleophilic centres of the two interacting molecules. A good linear correlation between the GEDT and the asynchronicity at eight of the TSs associated to the P-DA and I-DA reactions give in Figure 1 can be established, $R^2 = 0.95$ (see Figure S1 in Supplementary Material). As can be see, the asynchronicity increases with the increase of the polar character of the reaction; i.e., the increase of the GEDT at the TSs [13-15,32]; i.e. the stronger nucleophilic/electrophilic interactions at the TSs involving non-symmetric electrophiles, higher the asynchronicity is. As a consequence, I-DA reactions can take place through a non-concerted *two-stage one-step* mechanism [25] via a highly asymmetric TS [24], even though a two-step mechanism involving a cation intermediate [26]. The increase of the

Preprints (www.preprints.org) | NOT PEER-REVIEWED | Posted: 27 May 2021 doi:10.20944/preprints202105.0672.v1

asynchronicity enhances the distance between the ends of the two interacting frameworks, the iminium cation and the diene (see **TS-III** in Figure 2), and consequently, decrease the steric (Pauli) repulsions. Consequently, the decrease of steric (Pauli) repulsions is a consequence of the increase of the asynchronicity, and non-*vice versa*; asynchronicity in P-DA and I-DA reaction depends on the GEDT taking place at the TSs, which depends on the electrophilic/nucleophilic nature of the reagents.

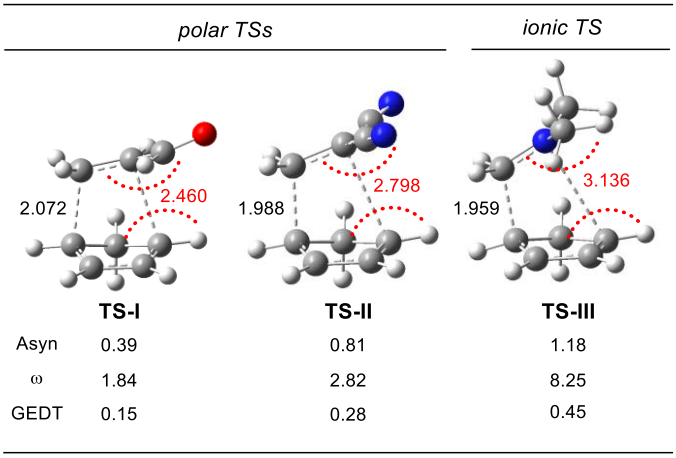

	TS-I	TS-II	TS-III
Asyn	0.39	0.81	1.18
ω	1.84	2.82	8.25
GEDT	0.15	0.28	0.45

Figure 2. B3LYP/6-32G(d) Asynchronicity, Asyn=d1-d2 in Angstroms Å, electrophilicity ω index of the ethylene, in eV, and GEDT, in e, at the TSs involved in P-DA reactions, **TS-I** and **TS-II**, and in I-DA reaction, **TS-III**.

Although I-DA reaction can be viewed as the extreme of the P-DA reactions [15], they have many different behaviours to P-DA reactions; i.e. I-DA reactions are poor *endo* selective, and polar solvents cause a contrary effect to in P-DA reactions. Herein, a complete MEDT study of I-DA reactions involving cationic species is presented. To this end, the I-DA reactions of six iminium cations, **6**, **15-19**, with Cp **1** were selected as computational models (see Scheme 5). It is interesting to remark that protonated imines **15** and **17** can be considered as species participating in acid Bronsted catalysed DA reactions of imines **13** and **14** [23].

The present MEDT study would like to respond to the following questions: (i) what is the origin of the high acceleration and asynchronicity found in I-DA reactions; (ii) which is the origin of the low *endo* selectivity in contrast with the high *endo* selectivity found in P-DA reactions; and (iii) what is the role of the solvent polarity in theses I-PA reaction.

Preprints (www.preprints.org) | NOT PEER-REVIEWED | Posted: 27 May 2021 doi:10.20944/preprints202105.0672.v1

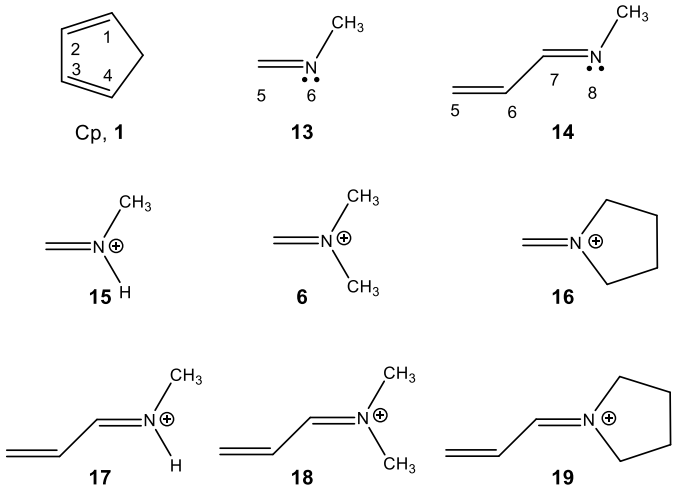

Scheme 5. Structures of the species involved in the P-D reactions of Cp **1** with imines **13** and **14**, and the I-DA reactions with iminium cation **6**, **15-19**.

3. Results and Discussions

The present MEDT study has been divided into three parts: i) first, a study of the electronic structure and reactivity at the ground state (GS) of the reagents is perfomed; ii) in the second part, the study of the potential energy surface of the I-DA reactions of iminium cations **6**, **15-19** with Cp **1** is carried out; and finally, iii) in the third part, a topological analysis of the bonding changes along the I-DA reactions is presented. The origin of the regioselectivity in I-DA reactions and asynchronicity in bond formation at the TSs is analysed in base on the changes of electron density.

3.1. Study of the electronic structure and reactivity at the ground state of the reagents.

3.1.1. Analysis of the electronic structure of imines and iminium cations.

In order to get information about how the formation of the iminium cations modifies the electronic structure of imines, an electron localisation function [33] (ELF) and natural population analysis [34,35] (NPA) analyses of imines **13** and **14**, and iminium cations **6** and **18** was first performed. The ELF valence basins localisation domains, the ELF-based Lewis-like structures and natural atomic charges are represented in Figure 3.

Preprints (www.preprints.org) | NOT PEER-REVIEWED | Posted: 27 May 2021 doi:10.20944/preprints202105.0672.v1

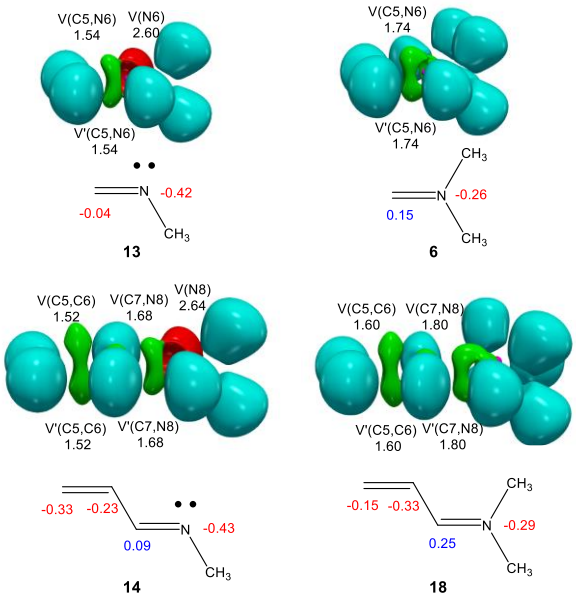

Figure 3. ωB97XD/6-311G(d,p) localisation domains (isosurface value = 0.75), blue colour is used to show protonated basins, red colour for the monosynaptic basins, green colour for the disynaptic basins and magenta colour for core basins, ELF based Lewis-like structures, and natural atomic charges, in average number of electrons e, blue colour is used for positive charges and red colour for negative ones, of imines **13** and **14**, and iminium cations **6** and **18**.

ELF of imine **13** shows the presence of two disynaptic basins, V(C5,N6) and V'(C5,N6) integrating a total of 3.08 e, one V(N6) monosynaptic basin, integrating 2.60 e, and one V(N6,C(Me)) disynaptic basin, integrating 1.74 e. The two disynaptic basins are associated to the underpopulated C5–N6 double bond, and the monosynaptic basin is associated to the non-bonding electron density of the N6 nitrogen. ELF of conjugated imine **14** shows the presence of two disynaptic basins, V(C5,C6) and V'(C5,C6) integrating a total of 3.04 e, one V(C6,C7) disynaptic basins, integrating 2.22 e, two disynaptic basins, V(C7,N8) and V'(C7,N8), integrating a total of 3.36 e, and one V(N8) monosynaptic basin, integrating 2.64 e. The two V(C5,C6) and V'(C5,C6) disynaptic basins are associated to the underpopulated C5–C6 double bond, the V(C6,C7) disynaptic basin is associated to the overpopulated C6–C7 single bond, the V(C7,N8) and V'(C7,N8) disynaptic basins are associated to the underpopulated C7–N8 double bond, and the monosynaptic basin is associated to the non-bonding electron density of the N8 nitrogen. In addition, one V(N8,C(Me)) disynaptic basin, integrating of 1.75 e, associated to the N8-C(Me) single bond is observed.

ELF of iminium cation **6** shows the presence of two disynaptic basins, V(C5,N6) and V'(C5,N6), integrating a total of 3.48 e, and two disynaptic basins, V(N6, C(Me))

Preprints (www.preprints.org) | NOT PEER-REVIEWED | Posted: 27 May 2021 doi:10.20944/preprints202105.0672.v1

and V(N6, C'(Me)), integrating 1.92 e each one. ELF of conjugated iminium cation **18** shows the presence of two disynaptic basins, V(C5,C6) and V'(C5,C6) integrating a total of 3.20 e, one V(C6,C7) disynaptic basins, integrating 2.22 e, and two disynaptic basins, V(C7,N8) and V'(C7,N8), integrating a total of 3.60 e. In addition, two disynaptic basins, V(N8, C(Me)) and V(N8, C'(Me)), integrating 1.88 e each one, are observed.

On the other hand, ELF of Cp **1**, non-represented in Figure 3, shows the presence of two disynaptic basin, V(C1,C2) and V'(C1,C2), integrating a total of 3.38 e, one V(C2,C3) disynaptic basin, integrating a total of 2.21 e, and two disynaptic basin, V(C3,C4) and V'(C3,C4), integrating a total of 3.38 e. The C1=C2–C3=C4 bonding region accumulate a total of 8.97 e.

The natural atomic charges are given in Figure 3. At imine **13**, while the C5 carbon has a negligible negative charge, the N6 nitrogen is negatively charged by 0.42e. At conjugated imine **14**, while the C5 and C6 carbons are negatively charged by 0.33 and 0.23 e, respectively, the C7 carbon is slightly positively charged by 0.09 e; the N8 nitrogen is negatively charged by 0.43. At iminium cation **6**, while the C5 carbon is positively charged by 0.15 e, the N6 nitrogen is negatively charged by 0.26e. At conjugated iminium **18**, while the C5 and C6 carbons are negatively charged by 0.15 and 0.33 e, respectively, the C7 carbon is slightly positively charged by 0.25 e; the N8 nitrogen is negatively charged by 0.29 e.

Some appealing conclusions can be drawn from the analysis of the electronic structure of imines **13** and **14** and iminium cations **6** and **18**: i) ELF of the C–C and C–N double bonds of imines **13** and **14** shows a depopulation of these bonding regions as a consequence of the polarisation of the molecular electron density towards the N nitrogen; note that the non-bonding region of the nitrogen integrates more that 2.60 e; ii) the populations of these bonding regions are higher at iminium cations **6** and **18** than at imines **13** and **14**. This finding is a consequence of the formation of the new C-C(Me) single bond, which are populated by lesser of 1.92 e. Consequently, the excess of the non-bonding nitrogen electron density of imines **13** and **14** is redistributed towards the C–C and C–N bonding regions of **6** and **18**; iii) the nitrogen centres of the iminium cations **6** and **18** are negatively charged, a behaviour against the positive charge represented at the Lewis structures of iminium cations. This behaviour is a consequence of the fact that in organic cationic species, the hydrogens are the centres who mainly support the positive charge; iv) analysis of the electronic structures of the conjugated imine **14** and iminium

Preprints (www.preprints.org) | NOT PEER-REVIEWED | Posted: 27 May 2021 doi:10.20944/preprints202105.0672.v1

cation **18** shows that the different substitution on the C5–C6 double bonds of these species does not modify substantially the electronic structure of the ethylene framework participating in these DA reactions; and finally, v) at the most electrophilic iminium cation **18**, the β-conjugated C5 carbon, which supports a negative charge of -0.15 e, is the most electrophilic center of this cationic species; see analysis of the electrophilic Parr functions. This finding supports the earlier observation that the electrophilicity and nucleophilicity cannot be related only with charge distribution at the GS of the molecules, but with the propensity of changes on electron density resulting of the GEDT along a polar reaction, which is anticipated by the analysis of the Parr functions [28].

3.1.2. Analysis of the CDFT reactivity indices at the GS of the reagents.

Many studied devoted to cycloaddition reactions have proof that the analysis of the global and local reactivity indices defined within the CDFT [18,19] is a powerful tool to understand polar reactions [36,37]. The CDFT indices were obtained at the B3LYP/6-31G(d) computational level due to it was used to define the scales of electrophilicity and nucleophilicity [19]. The global reactivity indices of imines **13** and **14**, iminium cations **6**,**15-19**, and Cps **1** and **20** are collected in Table 1.

Table 1. B3LYP/6-31G(d) Global reactivity indices, the electronic chemical potential, μ, chemical hardness, η, electrophilicity, ω, and nucleophilicity, *N*, in eV, of imines **8** and **9**, iminium cations **1-6**, and Cp **7**.

	μ	η	ω	*N*
17	-10.11	5.36	9.53	-3.67
15	-11.83	7.80	8.97	-6.61
19	-9.76	5.32	8.95	-3.30
18	-9.53	5.22	8.71	-3.02
6	-11.18	7.56	8.26	-5.84
16	-10.51	6.73	8.20	-4.75
14	-3.91	5.84	1.31	2.30
13	-3.46	6.80	0.88	2.26
Cp **1**	-3.01	5.48	0.83	3.37
CpMe **20**	-2.84	5.31	0.76	3.62

The electronic chemical potentials [18,38] μ of imines, μ = –3.46 (**13**) and –3.91(**14**) eV, are closer to that of Cp **1**, μ =–3.01 eV, indicating that the corresponding HDA

Preprints (www.preprints.org) | NOT PEER-REVIEWED | Posted: 27 May 2021 doi:10.20944/preprints202105.0672.v1

reactions will have non-polar character and high activation energies. On the other hand, the six iminium cations present very low electronic chemical potentials μ values, between –9.53 (**18**) and –11.83 (**15**) eV. Consequently, the corresponding I-DA reactions will experience a high GEDT and very low activation energies.

The electrophilicity ω index [16] of imines **13** and **14** is 0.88 and 1.31 eV, respectively, being classified as marginal electrophiles, while the nucleophilicity *N* values [17], 2.26 and 2.30 eV, classify they also as moderate nucleophiles. The presence of the electronegative N8 nitrogen in the heterodiene **14** decreases its nucleophilic character with respect to that of 1,3-butadiene, N = 2.93 e, Consequently, imines **13** and **14** will not participate neither as ethylene nor as diene in P-DA reactions.

The electrophilicity ω index of iminium cations, between 8.20 (**16**) and 9.53 (**17**) eV, classified they as strong electrophiles. These high values, higher than 4.0 eV, permit classified they as a superelectrophiles [21]. Consequently, they will participate in I-DA reactions with unappreciable activation energies. All iminium cations present negative nucleophilicity *N* indices.

The electrophilicity ω and nucleophilicity *N* indices of Cp **1**, 0.83 and 3.37 eV, permit its calcification as a moderate electrophile and a strong nucleophile. The inclusion of an electron-releasing methyl group on the C1 carbon of Cp **1** decrease the electrophilicity ω index of CpMe **20** to 0.76 eV and increases its nucleophilicity *N* index to 3.62 eV, thus, being classified as a marginal electrophile and a strong nucleophile.

From the electrophilicity ω indices of the iminium cations given in Table 1, some appealing conclusions can be obtained: i) the series of the conjugated iminium cations **17-19** are more electrophilic than iminium cations **6** and **16**. In spited of that, the later have lesser electronic chemical potentials μ; the softer character of the former makes they more electrophiles. Note that the softness S in the inverse of the hardness η, S = 1/η; ii) the protonated iminium cations are more electrophiles that the dialkyl derivative ones as a consequence of the electron-releasing character of the CH_3 and CH_2 groups; and finally, iii) a different behaviour have the two cyclic iminium cations. While the dimethyl derivative **6** is more electrophilic than cyclic **16**, cyclic iminium cation **19** is more electrophilic than the dimethyl derivative **18**.

DA reactions involving non-symmetric electrophilic compounds take place via asynchronous TSs. The most favourable two-center interactions between the two interacting species in polar process takes place between the most electrophilic center of

Preprints (www.preprints.org) | NOT PEER-REVIEWED | Posted: 27 May 2021 doi:10.20944/preprints202105.0672.v1

the electrophile, and the most nucleophilic center of the nucleophile [39]. In this context, the electrophilic P_k^+ and nucleophilic P_k^- Parr functions [28] derived from the excess of spin electron density reached via the GEDT [12] process from the nucleophile toward the electrophile have shown to be one of the most accurate and insightful tools for the study of the local reactivity in polar and ionic processes. The C1 and C4 carbons of Cp **7** are the most nucleophilic centres of this diene. In order to explain the asynchronicity in the C-C and C-N(C) bond formation, the electrophilic P_k^+ functions of imines **13** and **14**, and dimethyl iminium cations **6** and **18** were analysed. The corresponding values are given in Figure 4.

As expected, the C5 carbon of imine **13** and iminium cation **6**, P_k^+ = 0.65 and 0.84, respectively, are more electrophilically activated than de N6 nitrogen, P_k^+ = 0.41 and 0.25. Formation of iminium cation **6** increases the electrophilic activation of the C5 carbon, indicating that the corresponding TS will be more asynchronous.

The C5 carbon of conjugated imine **14**, P_k^+ = 0.48, is also the most electrophilic center of this species, followed of the N8 nitrogen, P_k^+ = 0.32. On the other hand, in spite of the strong electrophilic activation of the C7 carbon of iminium cation **18**, P_k^+ = 0.50, the C5 carbon remains as the most electrophilic center of this species, P_k^+ = 0.57. Note that the C6 carbon is electrophilically deactivated, –0.18, indicating that the corresponding TS will be highly asynchronous.

Preprints (www.preprints.org) | NOT PEER-REVIEWED | Posted: 27 May 2021 doi:10.20944/preprints202105.0672.v1

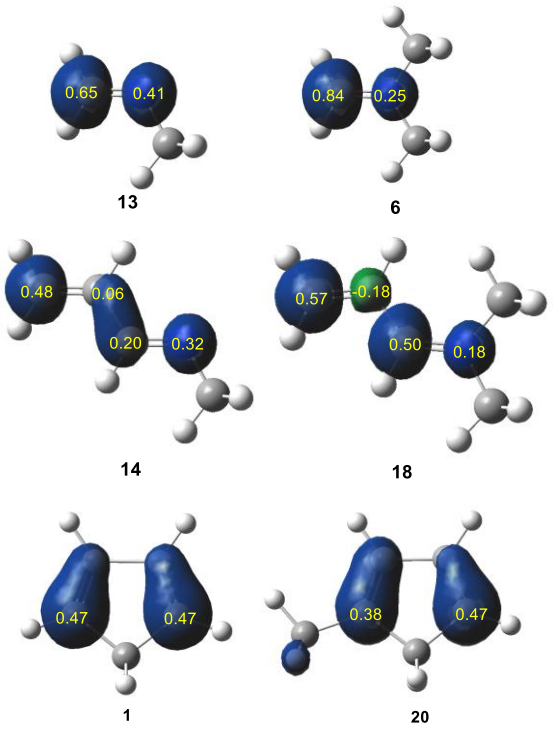

Figure 4. 3D representations of the Mulliken atomic spin densities of the radical anion of imines **13** and **14**, and neutral radical **6** and **18**, and the radical cation of Cp **1** and CpMe **20**, and the electrophilic P_k^+ and nucleophilic P_k^- Parr functions.

Analysis of the electrophilic P_k^+ Parr functions of these species indicates that the most favourable two-center interactions at the corresponding TSs will take place between one of the two end carbons of the symmetric diene Cp **1**, i.e. the C1 one, and the C5 carbon of these imine derivatives. Formation of the corresponding cation iminium increases the electrophilic activation of the C5 carbon with respect to the N6 or C6 centres, increasing the asynchronicity in the C-N(C) single bond formation.

It is interesting to remark the higher electrophilic activation of the C5 carbon of iminium cation **18**, P_k^+ = 0.57, than that of the C7 one P_k^+ = 0.50, in spite of that the C5 carbon is negatively charged, -0.15 e, while the C7 carbon is positively charged, 0.25 e (see Figure 3). This finding support the earlier assumptions that electrophilicity is not controlled by positive charged centres [21,40].

Analysis of the nucleophilic P_k^- Parr functions of Cp **1** indicates that the C1 and C4 are symmetrically activated. These carbons are the most nucleophilic centre of Cp, P_k^- = 0.47. The inclusion of an ER –Me at the C1 carbon does not modify the nucleophilic P_k^- Parr function at the C4 carbon, P_k^- = 0.47, but relocates the nucleophilic P_k^- Parr

Preprints (www.preprints.org) | NOT PEER-REVIEWED | Posted: 27 May 2021 doi:10.20944/preprints202105.0672.v1

function at the C1 and C2 carbons. Consequently, the C4 carbon becomes the most electrophilic center of CpMe **20**.

3.2. Study of the potential energy surface of I-DA reactions.

*3.2.1. study of the I-DA reactions of iminium cations **6,15-19** with Cp **1***

While for the symmetric iminium cations **6** and **16** only one reaction path is feasible, for the non-symmetric iminium cations **15**, **17**, **18** and **19**, two stereoisomeric reaction paths are feasible: the *endo* and the *exo*. In addition, due to the presence of two double bonds, C–C and C–N, in the iminium cations derived from imine **14**, the chemoisomeric reaction path associated to the attack of Cp **1** to the C7–N8 double bond of iminium cation **18** was also considered (see Scheme 6). The stationary points involved in the six I-DA reactions, are given in Scheme 6, while the relative energies in acetonitrile are given in Table 2. Note that due to the high instability of gas phase cationic species, the relative energies are analysed in acetonitrile. Thus, while acetonitrile stabilizes the neutral Cp **1** by 7.7 kcal·mol^{-1}, iminium cation **15** is stabilized by 53.7 kcal·mol^{-1}. In other to understand the behaviours of these I-DA reactions, the DA reactions of imines **13** and **14** with Cp **7** were also studied (see Section 1 in Supplementary Material).

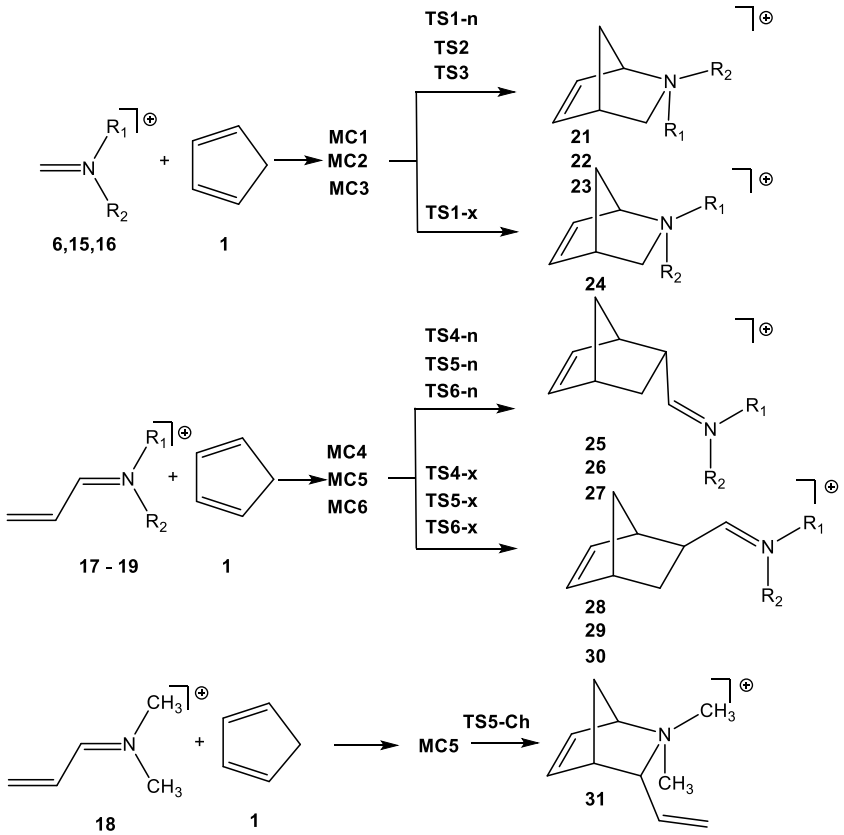

Scheme 6. I-DA reactions of iminium cations **6**, **15-19** with Cp **1**.

Preprints (www.preprints.org) | NOT PEER-REVIEWED | Posted: 27 May 2021 doi:10.20944/preprints202105.0672.v1

At the begin of the reactions, a series of molecular complex can be found. They are characterised by the presence of weak electronic interactions between Cp **1** and the iminium cations. For each of these I-DA reactions, only the most stable MC was selected as energy reference. The MCs are found between 5.6 (**MC4**) and 7.2 (**MC3**) kcal·mol^{-1} more stable than the separated reagents. The relative energies of the TSs with respect to the separated reagents associated to these I-DA reactions are found between –0.6 (**TS1-n**) and 4.4 (**TS4-x**) kcal·mol^{-1}; the reactions being exothermic between 24.0 (**22**) and 28.4 (**21**) kcal·mol^{-1}.

Some appealing conclusions can be drawn from these energy results given in Table 2: i) formation of MCs are exothermic processes, lesser than 7.2 (**MC3**) kcal·mol^{-1}. However, if the thermal correction and the entropies are considered, they become exergonic (see later); ii) considering these MCs, the activation energies associated to these I-DA reactions are found between 6.0 (**TS1-n**) and 10.0 (**TS3**) kcal·mol^{-1}. These activation barriers are between 13 and 20 kcal·mol^{-1} lower in energy that those associated to the DA reactions of neutral imines **13** and **14** with Cp **1** (see Scheme S1 in Supplementary Material); iii) these I-DA reactions present low *endo* stereoselectivity; the energy difference between the *endo*/*exo* TSs is lesser than 1.2 kcal·mol^{-1} (**TS1-n**). The *endo* selectivity decreases with the increase of the activation energy; iv) the reaction of Cp **1** with iminium cation **18** is completely chemoselective as **TS5-Ch** is found 7.7 kcal/mol above **TS5-n**. This high energy difference permits to discard the attach of Cp **1** on the C7–N8 double bond iminium cations **17-19**; v) these I-DA reactions are highly exothermic, higher than 24.0 (**22**) kcal·mol^{-1}. Consequently, these cycloaddition reactions can be considered irreversible (see later); and finally, vi) formation of **31** is exothermic by 15.3 kcal·mol^{-1}. Consequently, the attach of Cp **1** on the C7–N8 double bond iminium cation **18** is both kinetically and thermodynamically disfavoured with respect to the attach to the C5-C6 double bonds.

Table 2. ωB97XD /6-311G(d,p) relative electronic energies in acetonitrile, kcal·mol^{-1}, of the stationary points involved in the I-DA reactions of iminium cations **6**, **15-19** with Cp **1**.

15		**6**		**16**	
MC1	-6.6	**MC2**	-6.6	**MC3**	-7.2
TS1-n	-0.6	**TS2**	2.9	**TS3**	2.8
TS1-x	0.6				
21	-28.4	**22**	-24.0	**23**	-24.6
24	-28.1				

Preprints (www.preprints.org) | NOT PEER-REVIEWED | Posted: 27 May 2021 doi:10.20944/preprints202105.0672.v1

17		18		19	
MC4	-5.6	**MC5**	-5.6	**MC6**	-5.8
TS4-n	3.7	**TS5-n**	3.1	**TS6-n**	3.7
TS4-x	4.4	**TS5-x**	3.6	**TS6-x**	4.1
		TS5-Ch	10.8		
25	-28.3	**26**	-28.3	**27**	27
28	-27.7	**29**	-27.7	**30**	-27.7
		31	-15.3		

In P-DA reaction, the *endo* selectivity increased with the increase of the polar character of the reaction, resulting of the GEDT taking place at the TSs [13]. The GEDT increases the zwitterionic character of the TSs, increasing the favourable electrostatic interactions appearing between the ends of the two interacting frameworks along the *endo* approach mode. However, in I-DA reactions, the GEDT provokes a redistribution of the electron density, thus, appearing positive charges at the two interacting frameworks, and consequently, presenting low *endo* selectivity

The geometries of the more favourable *endo* TSs associates to these I-DA reactions are given in Figure 5. The geometries of the *exo* TSs are given in Figure S4 in the Supplementary Material. The distances between the C1–C5 and C4–N6 interacting centers at the TSs of the I-DA reactions of iminium cations **6**, **15** and **16** in acetonitrile are: 1.995 and 2.869 Å at **TS1-n**, 1.965 and 2.875 Å at **TS2**, and 1.931 and 3.049 Å at **TS3**, while those between the C1–C5 and C4–C6 interacting centers at the TSs of the I-DA reactions of conjugated iminium cations **17 - 19** are: 2.019 and 2.832 at Å **TS4-n**, 2.019 and 2.831 Å at **TS5-n**, and 2.012 and 2.819 at Å **TS6-n**. Some appealing conclusions can be drawn from these geometrical parameters: i) these distances indicate that these TSs are associated to highly asynchronous single bond formation process. They are associated to a two-center interaction between the most nucleophilic center of Cp **1**, the C1 carbon, and the most electrophilic center of these iminium cations, the C5 carbon, a behaviour anticipated by analysis of the electrophilic Parr functions; ii) for the two series of I-DA reactions there is a decrease of the C1–C5 distance with the increase of the activation energy; for these series, the most favourable TS more delayed is. This finding can be understand as an application of the Hammond principle [41]; and finally, iii) the comparison the gas phase and in acetonitrile geometries indicates that there is not a remarkable change with the inclusion of solvent effects on the gas phase geometries. The differences of the C1–C4 distances at the six TSs are lesser than 0.06 Å. These results

Preprints (www.preprints.org) | NOT PEER-REVIEWED | Posted: 27 May 2021 doi:10.20944/preprints202105.0672.v1

point out that while the inclusion of solvent effects modifies substantially the energies, it does not change the electronic structure of the TSs (see later).

Herein, it is interesting to remark that unlike the P-DA reactions in which the TSs have a zwitterionic character resulting from the GEDT, at the TSs associated with I-DA reactions, both frameworks are positively charged. These behaviours have an important experimental consequence; while in P-DA reaction, polar solvent accelerate the reactions by a better solvation of the zwitterionic TSs than reagents, in I-DA reactions, solvent effect deaccelerate them by a better solvation of the cationic reagent than TSs.

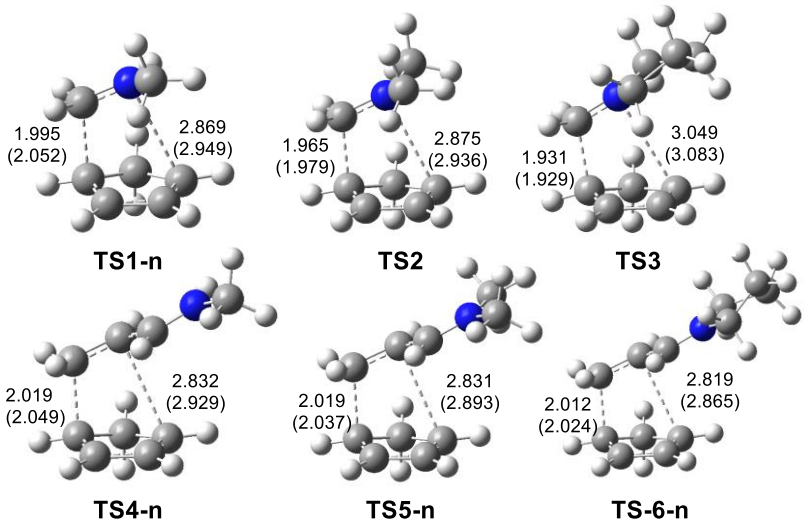

Figure 5. ωB97XD/6-311G(d,p) geometries of the *endo* TSs for DA reactions of iminium cations **6**, **15-19** with Cp **1**. The C–C C–N distance are given in Angstroms. The gas phase distances are given in parenthesis.

The ionic nature of these I-DA reactions was evaluated by computing the GEDT at the gas phase TSs. The computed GEDT values at the corresponding TSs, which fluxes from the nucleophilic Cp **1** to the superelectrophilic iminium cations is: 0.40e (**TS1-n**), 0.43 e (**TS1-x**), 0.43 e (**TS2** and **TS3)**, 0.37 e (**TS4-n**), 0.39 e (**TS4-x**), 0.38 (**TS5-n** and **TS5-x**), 0.38 e (**TS6-n**) and 0.37 (**TS6-x**). These very high values point out the high GEDT taking place at these I-DA reactions. Note that at the DA reactions involving neutral imines, the GEDT is lower than 0.15 e (see Section 1 in Supplementary Material). As expected, the GEDT values at the TSs associated to the I-DA reactions involving the most electrophilic iminium cations **6**, **15** and **16** is slightly higher than those involving unsaturated iminium cations **17** – **18**. The GEDT at the TSs in acetonitrile are very closer to those obtained in the gas phase; thus, the GEDT values of **TS1-n** and **TS2** in acetonitrile are 0.41e and 0.43 e, respectively. As expected, in these I-DA reactions the

Preprints (www.preprints.org) | NOT PEER-REVIEWED | Posted: 27 May 2021 doi:10.20944/preprints202105.0672.v1

electron density fluxed form Cp **1** towards the iminium cations, theses reactions being classified as the forward electron density flux (FEDF) [42].

As shows Figure 6, a good linear correlation between the GEDT and the asynchronicity at the TSs of the DA reaction of imines **13** and **14** and the I-DA reaction of cations **6**, **15-19** can be established (R^2 = 0.98). Thus, while the low polar DA reactions of neutral imines **13** and **14**, GEDT < 0.15 e, present low asynchronous TSs, Δl < 0.2 Å, the I-DA reactions of iminium cations **6**, **15-19** with a GEDT > 0.37 e present highly asynchronous TSs, Δl > 0.8 Å. These behaviours are a consequence of fact that while low polar DA reactions of neutral imines are associated to a low asynchronous four-center interactions, the I-DA reactions of non-symmetric iminium cations are associated to high asynchronous two-center interactions. These finding account for the decrease of the steric (Pauli) repulsion with the increase of the ionic character of the reaction.

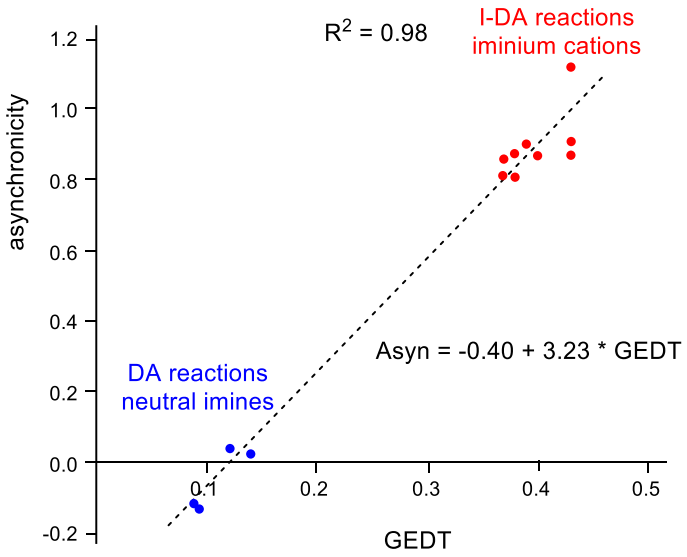

Figure 6. Plot of the asynchronicity, Asyn=(l1 - l2) in Angstroms, vs the GEDT, in e, taking place at the TSs associated to the DA reaction of non-symmetric imines and the I-DA reaction of non-symmetric iminium cations.

3.2.2. Study of the regioselectivity in I-DA reactions.

Due to the symmetry of Cp **1**, these I-DA reactions do not have regioisomeric reaction path. In order to analyse the regioselectivity in I-DA reactions, the reaction of iminium cation **6** with CpMe **20** was also considered (see Scheme 7). Dues to the symmetry of iminium cation **6** only to competitive regioisomeric reaction paths, named *ortho* and *meta*,

Preprints (www.preprints.org) | NOT PEER-REVIEWED | Posted: 27 May 2021 doi:10.20944/preprints202105.0672.v1

are feasible. The stationary points involved in this I-DA reaction are given in Scheme 7, while the relative energies in acetonitrile are given in Table 3.

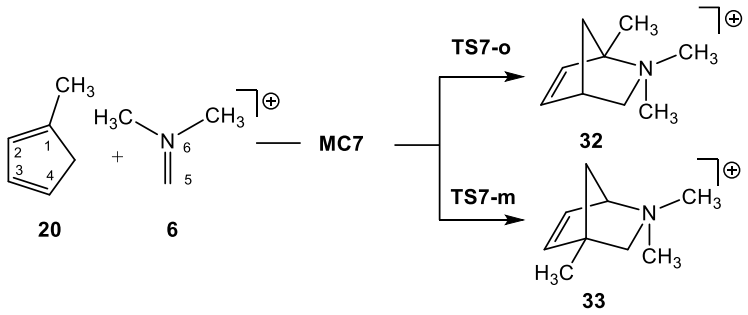

Scheme 7. I-DA reaction of iminium cations **6** with CpMe **20**.

The relative energies of the TSs with respect to the separated reagents are –0.8 (**TS7-o**) and 2.7 (**TS7-m**) kcal·mol^{-1}; the reaction being exothermic by 24.3 (**32**) and 24.1 (**33**) kcal·mol^{-1}. If the formation of **MC7** is considered, the activation energies associated to the two regioisomeric reaction paths becomes 6.7 (**TS7-o**) and 10.2 (**TS7-m**) kcal·mol^{-1}. Consequently, this I-DA reaction is completely regioselective as **TS7-m** is found 3.5 kcal·mol^{-1} above **TS7-o**. The activation energy associated to this I-DA reaction is 2.8 kcal·mol^{-1} lower in energy than that involving Cp **1** via **TS2** as a consequence of the more nucleophilic character of CpMe **20** than Cp **1** (see Tables 1 and 3).

Table 3. ωB97XD /6-311G(d,p) relative electronic energies in acetonitrile, kcal·mol^{-1}, of the stationary points involved in the I-DA reaction of iminium cation **6** with CpMe **20**.

MC7	-7.5
TS7-o	-0.8
TS7-m	2.7
32	-24.3
33	-24.1

The geometries of the two regioisomeric TSs associates to this I-DA reaction are given in Figure 7. The distances between the C1–C5 and C4–N6 interacting centers at the TSs of the I-DA reaction of iminium cation **6** with CpMe **20** in acetonitrile are: 2.031 and 2.989 Å at **TS7-o** and 1.967 and 2.780 Å at **TS7-m**. These distances indicate that these TSs are associated to high asynchronous single bond formation processes which are controlled by the most electrophilic C5 carbon of iminium cation **6**. The more favourable regioisomeric **TS7-o** is associated to the two center interaction between the most

Preprints (www.preprints.org) | NOT PEER-REVIEWED | Posted: 27 May 2021 doi:10.20944/preprints202105.0672.v1

electrophilic center of iminium cation **6** and the most nucleophilic center of CpMe **20**, the non-substituted C4 carbon, a behaviour anticipated by the analysis of the Parr Functions (see Figure 4).

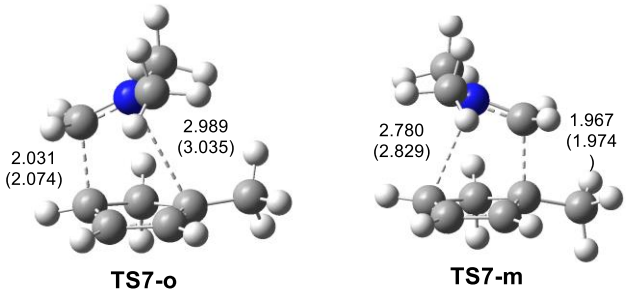

Figure 7. ωB97XD /6-311G(d,p) geometries of two regioisomeric TSs for I-DA reaction of iminium cation **6** with CpMe **20**. The distances are given in Angstroms. The gas phase distances are given in parenthesis.

At the two regioisomeric TSs, the GEDT taking place from Cp framework to the iminium cation one is 0.40 e at **TS7-o** and 0.44 e at **TS7-m**. These very high values point out the high ionic character of this I-DA reaction. The GEDT at the more unfavourable **TS7-m** is higher than that at **TS7-o** as a consequence of the more advanced character of the former [43]. On the other hand, the high GEDT taking place at the TSs involving the non-symmetric iminium cation **6** accounts of the high asynchronicity found in this I-DA reaction.

*3.2.3 Thermodynamic analysis of the I-DA reaction of iminium cation **6** with Cp **1***

The thermodynamic data of the reaction of iminium cation **6** with Cp **1**, as a representative I-DA reaction of this series, were analysed. Relative enthalpies and Gibbs free energies, computed at 25 ºC in acetonitrile, are given in Figure 8.

Inclusion of the thermal corrections to the electronic energies in acetonitrile decreases the relative enthalpies between 1.1 and 4.2 kcal·mol^{-1}. The lowers incidence takes place in the relative enthalpy of **TS2** which decreases by 1.1 kcal·mol^{-1} with respect to the electronic energy in acetonitrile. The inclusion of the thermal correction and entropies to enthalpies increases the relative Gibbs free energies between 10.5 and 15.9 kcal·mol^{-1} as a consequence of the unfavourable activation entropy associated to these bimolecular processes, between –35.2 and –53.3 cal·mol^{-1}·K^{-1}. Thus, the activation Gibbs free energy associated to the I-DA reaction of iminium cations **6** with Cp **1** in acetonitrile rise to 17.4 kcal·mol^{-1}, while formation of **22** becomes exergonic by only –4.0 kcal·mol^{-}

Preprints (www.preprints.org) | NOT PEER-REVIEWED | Posted: 27 May 2021 doi:10.20944/preprints202105.0672.v1

[1]. It is important to remark that while formation of **MC2** is an exothermic process, it is endergonic as a consequence of the unfavourable positive entropy associated to its formation (see Figure 8).

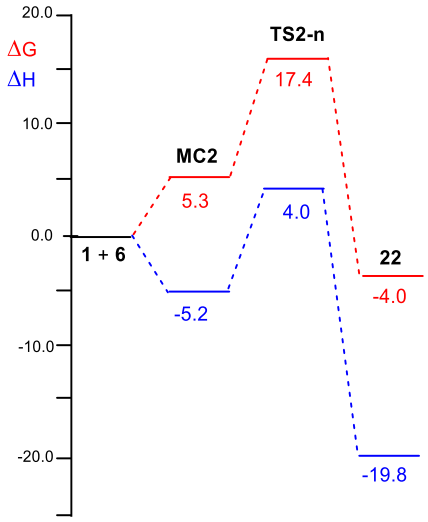

Figure 8. ωB97XD/6-311G(d,p) enthalpy, in blue, ΔH in kcal mol^{-1}, and Gibbs free energy, in red, ΔG in kcal mol^{-1}, profiles, in acetonitrile at 25 °C, for the I-DA reaction of iminium cation **6** with Cp **1**.

3.3. Topological analysis of the bonding changes along the I-DA reactions

MEDT establishes that the energy costs for the bonding charges along a chemical reaction are responsible for its feasibility. On the other hand, the comparative topological analysis of the electronic structures of TSs involved in the related reactions allows to characterize the similitudes or differences between them.

*3.3.1. ELF analysis of the C–C and N–C single bond formation along I-DA reaction of Cp **1** with iminium cation **6***

In order to understand the bonding charges along I-DA reactions, an BET study of the I-DA reaction of Cp **1** with iminium cation **6** was performed. The detailed BET study of this I-DA reaction is given in Section 2 in Supplementary Material. Some appealing conclusions can be obtained from this BET analysis: i) the energy cost (EC) associated to formation of **TS2**, which is found at *Phase III*, 2.2 kcal·mol^{-1}, is mainly associated with the depopulation of the C5–N6 bonding region of the iminium moiety from 3.65 to 3.10

Preprints (www.preprints.org) | NOT PEER-REVIEWED | Posted: 27 May 2021 doi:10.20944/preprints202105.0672.v1

e. Thus, the activation energy of this I-DA reaction can be related to the EC associated with the rupture of the C5–N6 double bond of iminium cation **6**; ii) the bonding changes associated to this I-DA reaction are very similar to those found in P-DA reactions, but they are more advanced in I-DA reactions; note that while in P-DA reactions the formation of the first C–C single bond takes place usually after to pass the TSs, in this I-DA reaction it takes place before to reach **TS2**. Note that at **TS2,** the C1–C5 single bond is already formed; iii) although the C5 carbon of iminium cation **6** is the most electrophilic center of this molecule, the electron density coming from both the initial depopulation of C5–N6 bonding region and that the GEDT is mainly accumulated at the N6 nitrogen first. Likewise, the bonding changes at the Cp framework are non-symmetric, the changes in the C1–C2 bonding region are more advanced than those in the C3–C4 one. This behaviour is a consequence of changes in electron density demanded for the formation of the first C1–C5 single bond; iv) formation of the first C1–C5 single bond takes place at **TS2**, at a C–C distance of ca. 1.98 Å and with an initial population of 0.76 e, by sharing the non-bonding electron density of two C1 and C5 *pseudoradical* centers (62:38) created from the rupture of the corresponding multiple bonds along the reaction path before reaching the TS [12];v) formation of the second C4–N6 single bond takes place at a C–N distance of ca. 2.11 Å and with an initial population of 1.71 e, mostly through the donation of the non-bonding electron density of the N6 nitrogen developed from the rupture of the C5–N6 double bond of **6** to the C4 carbon (96:4); and vi) this highly asynchronous I-DA reaction takes place through a marked non-concerted *two-stage one-step* mechanism [25] in which the formation of the second C4–N6 single bond takes place when the formation of the first C1–C5 one is almost completed (94 %).

*3.3.2. Comparative ELF analysis of the TSs involved in the DA reaction of Cp **1** with imines **13** and **14**, and those involved in the I-DA reaction of Cp **1** with iminium cations **6** and **18**.*

Finally, a comparative ELF topological analysis of the TSs involved in the DA reaction of Cp **1** with imine **13**, **TS7-n**, and unsaturated imine **14**, **TS8-n**, and those involved in the DA reaction of Cp **1** with iminium cation **6**, **TS2**, and unsaturated iminium cation **18**, **TS5-n** was performed in order understand the changes at the TSs of I-DA reactions with respect to those participating in P-DA reactions. The ELF attractors, with the most significant valence basin populations, are given in Figure 9.

Preprints (www.preprints.org) | NOT PEER-REVIEWED | Posted: 27 May 2021 doi:10.20944/preprints202105.0672.v1

The comparative analysis of the ELF of the polar **TS7-n**, **TS8-n** and ionic **TS-5n** indicates that they present a great similitude. They show the presence of one V(C1) monosynaptic basin, integrating 0.38 e, 0.29 e and 0.38 e, respectively, and one V(C5) monosynaptic basin, integrating 0.30 e, 0.25 e and 0.19 e. These monosynaptic basin, which have been created along the reactions paths, will be required for the subsequent C1–C5 single bond formation [12]. At these TSs, one V(C5,C[N]6) disynaptic basin is observed, with a populations of 2.46 e, 2.98 e and 2.73 e, respectively, as a consequence of a slight depopulation of the C–C[N] bonding region. On the other hand, the C1–C2–C3–C4 bonding regions of these TSs are characterised by the presence of three disynaptic basins, V(C1,C2), V(C2,C3) and V(C3,C4), integrating a total of 8.36 e (**TS7-n**), 8.46 (**TS8-n**) and 8.15 e (**TS5-5**), respectively. A significant part of the electron density lost in these frameworks, with respect to that of Cp **1**, 8.97 e, is involved in the formation of the V(C1) monosynaptic basins presents at these TSs.

A different behaviour is observed at **TS2**. Instead of the two V(C1) and V(C5) monosynaptic basins present at the other three TSs, a new V(C1,C5) disynaptic basin, integrating 0.76 e, is observed. The presence of this disynaptic basin indicates that at **TS2**, the formation of the new C1–C5 single bond has begun already. Considering that the formation of the C–C single bonds takes place in the sort range of 2.0 – 1.9 Å [12], this different behaviour of **TS2** with respect to the other three TSs is a consequence of its more advanced character. On the order hand, the C1–C2–C3–C4 and C5–C6 bonding regions of **TS2** are very similar to those at **TS5-n**.

Preprints (www.preprints.org) | NOT PEER-REVIEWED | Posted: 27 May 2021 doi:10.20944/preprints202105.0672.v1

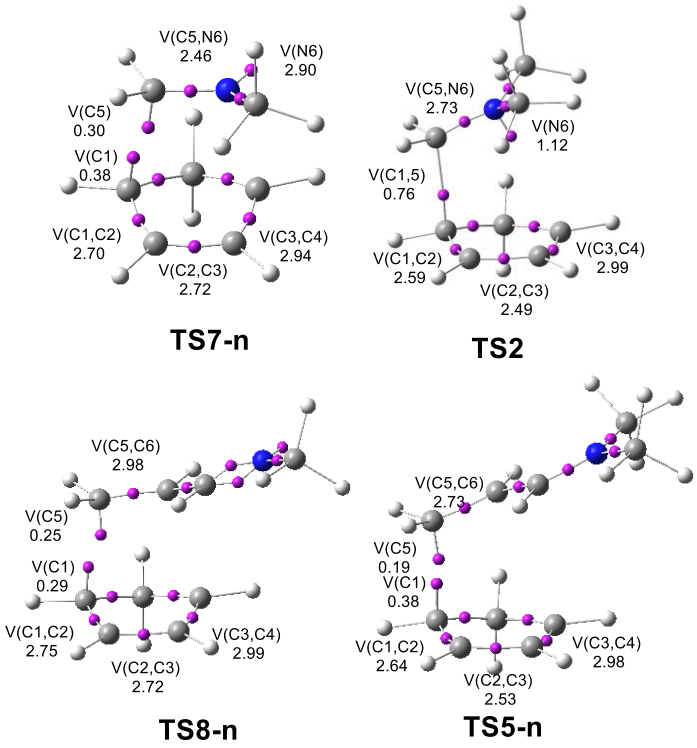

Figure 9. ELF basin attractor positions, with the most significant valence basin populations, of the TSs involved in the DA reaction of Cp **1** with imine **13**, **TS7-n**, and unsaturated imine **14**, **TS8-n**, and those involved in the DA reaction of Cp **1** with iminium cation **6**, **TS2**, and unsaturated iminium cation **18**, **TS5-n**.

From this ELF comparative analysis, it is possible to conclude that the four TSs belonging to P-DA reactions of imines and I-DA reactions of iminium cations, present similar electronic structures. Considering the similitude of the ethylenic C5-C[N]6 regions of these TSs, the very low activation energies associated to these I-DA reactions with respect to those of the P-DA reactions of imines **13** and **14**, between 15 and 23 kcal·mol^{-1}, can be related to the high GEDT taking place at the TSs of these I-DA reactions which favour the changes of electron density along the corresponding reaction paths [44].

3.3.3. Analysis of the origin of the regioselectivity in I-DA reactions

Many theoretical studies of cycloaddition reactions participating non-symmetric electrophilic species have established that the most favourable reaction path is that involving the two-center interaction between the most nucleophilic center of the nucleophile and the most electrophilic center of the electrophile species [39]. These favourable interactions, which facilitate the creation of the first C–C single bonds, control the regio- and the chemoselectivity in polar reactions as well as the asynchronicity in the

Preprints (www.preprints.org) | NOT PEER-REVIEWED | Posted: 27 May 2021 doi:10.20944/preprints202105.0672.v1

single bond formation. In order to assert these finding in I-DA reactions, a topological analysis of the regioisomeric **TS7-o** and **TS7-m** was performed. The ELF attractors, with the most significant valence basin populations, are given in Figure 10.

As can be seen, both regioisomeric TSs present a similar ELF structure. At the iminium cation framework, both TSs present two monosynaptic basins, VC5) and V(N6), integrating 0.20 e and 0.92 at **TS7-o** and 0.34 and 1.19 e at **TS7-m**, respectively. Note that the populations of these monosynaptic basins are higher at the more unfavourable **TS7-m** because of it is more advances (see Figure 10). On the other hand, the population of the V(C5,N6) disynaptic basin at **TS7-o** , 2.91 e, and at **TS7-m**, 2.65 e, indicates that the C5–N6 bonding region of iminium cation **6** has experienced a strong depopulations in other to create the V(N6) monosynaptic basin. Note that the population of this bonding region at iminium cation **6** is 3.48 e.

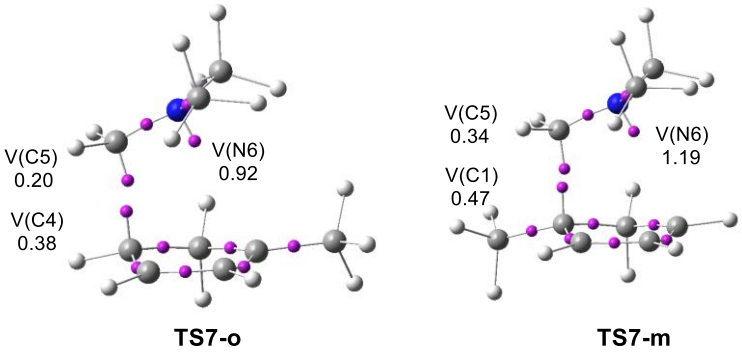

Figure 10. ELF basin attractor positions, with the most significant valence basin populations, of the regioisomeric TSs **TS7-o** and **TS7-m** involved in the I-DA reaction of CpMe **20** with iminium cation **6**.

At the diene frameworks, while the most favourable **TS7-o** shows the presence of a V(C4) monosynaptic basins, integrating 0.38 e, at the most nucleophilic C4 carbon of CpMe **20** (see Figure 10), **TS7-m** presents a V(C1) monosynaptic basins, integrating 0.47 e at the substituted C1 carbon. On the order hand, the total electron density of the C1–C2–C3–C4 bonding region of the Cp framework is 8.2 e at **TS7-o** and 8.1 e at **TS7-m**. Note that the total electron density of this bonding region at CpMe **20** is *ca* 9.0 e.

Consequently, at the more favourable **TS7-o**, the V(C4) monosynaptic basins demanded for the asynchronous formation of the first C4–C5 single bond is created at the most electrophilic center of CpMe **20**, the C4 carbon, which corresponds to the carbon of

Preprints (www.preprints.org) | NOT PEER-REVIEWED | Posted: 27 May 2021 doi:10.20944/preprints202105.0672.v1

CpMe **20** that loss less electron density along the GEDT process, a behaviour anticipated by analysis of the nucleophilic P_k^- Parr functions (see Figure 4) [28].

3.4. Origin of the asynchronicity in I-DA reactions

Several studied have evidenced the origin of the high asynchronicity found in the single bond formation in polar cycloaddition reactions [14,39]. These studies emphasised that the high asynchronicity is a consequence of the two-center interactions between the most nucleophilic centre of the nucleophile, and the most electrophilic center of the non-symmetrically substituted electrophilic species [14,39]. Note that many highly asynchronous TSs associated to P-DA reactions have been associated to Michael-type additions [43,45].

Because highly P-DA and I-DA reactions are associated to a two-center interactions, the two terminal centres that do not participate in the formation of the first single bond are not interacting. Note that at high asynchronous TSs, the C4 carbon of Cp **1** remains sp^2 hybridised. As a consequence, along the approach of the superelectrophilic iminium cations to the nucleophilic Cp **1** three stereoisomeric TSs can be feasible in I-DA reactions, two *gauche* and one *anti* (see Figure 11). They are related with the C2–C1–C5–C(N)6 dihedral angle at the TSs; thus, **TS2**, with is associated with the *gauche 60* approach mode, presents a C2–C1–C5–N6 dihedral angle of 68.4 angles.

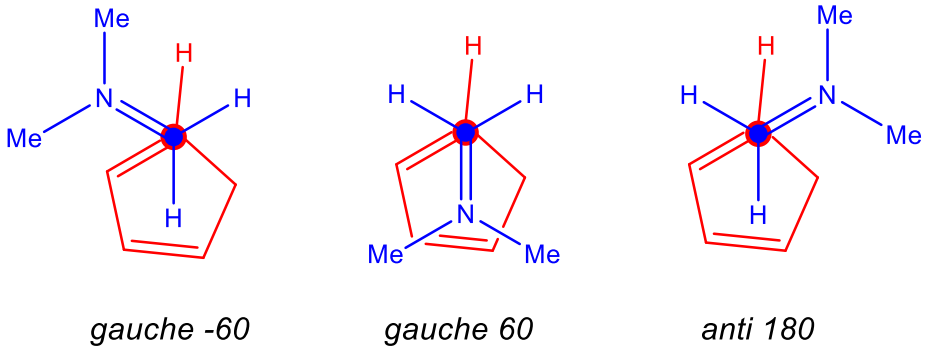

Figure 11. Three feasible stereoisomeric reaction paths associated to the C4 and C5 two-center interaction in the I-DA reaction of Cp **1** with iminium cation **6**.

Thus, along the approach of Cp **1** to iminium cation **6**, it is possible to find the *anti* 180 TS, **TS2-anti**, in which the C2–C1–C5–N6 dihedral angle is –162.3 degrees (see Figure 12). The corresponding stepwise *anti 180* reaction path is not competitive with the one-step *gauche* 60 one as **TS2-*anti*** is found 3.6 kcal·mol^{-1} above **TS2**. The GEDT at

Preprints (www.preprints.org) | NOT PEER-REVIEWED | Posted: 27 May 2021 doi:10.20944/preprints202105.0672.v1

TS2-*anti*, 0.48 e, is higher than that at **TS2**, 0.43 e, as a consequence of the shorter distance between the two frameworks at **TS2-*anti***, 1.839 Å. Note that the GEDT depends on the electrophilic/nucleophilic character of the reagents and the distance between the two interacting frameworks [43].

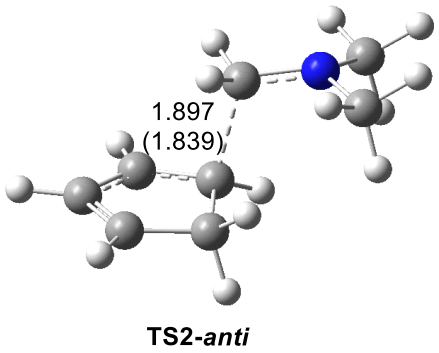

Figure 12. ωB97XD /6-311G(d,p) geometry of the stereoisomeric **TS-*anti*** for I-DA reaction of iminium cation **6** with Cp **1**. The distances are given in Angstroms. The gas phase distances are given in parenthesis.

TS2 and **TS2-*anti*** are two stereoisomeric species. However, while **TS2** is associated to a high asynchronous TS, the stereoisomeric **TS2-*anti***, cannot be characterised as a high asynchronous TS as it is associated to the first step of a stepwise I-DA reaction. These stereoisomeric TSs are associated with a similar C1–C5 single bond formation process. The unique relevant difference between both stereoisomeric TSs is the arrangement of the non-bonding electron density of the N6 nitrogen (see Figure S5 in Supplementary Material). Interestingly, while at the *gauche 60* **TS2** the two methyl groups of the iminium cation **6** are located above the hydrocarbon ring of Cp **1,** at the *anti 180* **TS2-*anti*** they are far.

It appears that the favourable electronic interactions present between the non-bonding electron density created at the N6 nitrogen along the reaction path and the C2–C3–C4 allylic framework of Cp **1**, which is positively charged, and not the steric repulsions associated to steric (Pauli) repulsions between the two interacting frameworks, which will be higher at the more favourable *gauche 60* **TS2** than at *anti 180* **TS2-*anti***, such has been suggested [29], will be responsible for the higher stability of **TS2** than **TS2-*anti***. Consequently, it appears that steric repulsions do not control nothing.

It can be concluded that the observed decrease of the steric repulsion with the increase of the nucleophilic/electrophilic interactions is a consequence of the increase of the asynchronicity resulting of an increase of the favourable two-center interactions

Preprints (www.preprints.org) | NOT PEER-REVIEWED | Posted: 27 May 2021 doi:10.20944/preprints202105.0672.v1

taking place at the polar and ionic TSs involving asymmetric electrophilic species caused by the GEDT. Therefore, the reduction of the steric (Pauli) repulsions characterised by Bickelhaup et al. after using an EDA analysis [29], is a consequence of the increase of the asynchronicity, which increase the distance between the ends of the two interacting frameworks, and never *vice versa*.

4. Conclusions

The behaviours of the I-DA reactions have been investigated within the MEDT at the ωB97XD/6-311G(d,p) computational level. To this end, the P-DA reactions of two imines **13** and **14**, and the I-DA reactions of six iminium cations **6**, **13**-**19** with Cp **1** have been investigated.

ELF topological analysis of these aza derivatives shows that the double bonds of both imines and iminium cations are very similar. Interestingly, the populations at the double bonds of iminium cations are slightly higher than at imines as a consequence of the reorganisation of the non-bonding electron density of the N nitrogen present in imines.

The superelectrophilic character of iminium cations, ω > 8.20 eV, accounts for the high reactivity of these species with respect to that of the corresponding neutral imines, ω < 1.31 eV, participating in P-DA reactions. Analysis of the electrophilic P_k^+ Parr functions at the iminium cations characterises the most electrophilic center of these species, thus accounting for the high regioselectivity and high asynchronicity found in these I-DA reactions.

The activation energies of the I-DA reactions are found between 13 and 20 kcal·mol^{-1} lower in energy than those associated to the DA reactions of neutral imines. These I-DA reactions are low *endo* selective as a consequence of the cationic character of the TSs, but highly regioselective.

Unlike P-DA reactions, polar solvents have a poor effect on the relative energies, and an unappreciable effect in the geometries. Interestingly, in solution the activation energies increase slightly as a consequence of the better solvation of the cationic iminium that TSs.

ELF topological analysis of the bonding changes along the I-DA reaction of iminium cation **6** with Cp **1** shows that the C–C single bond formation takes place at **TS2** at a C–C distance of ca. 1.98 Å and with an initial population of 0.76 e, by sharing the non-bonding electron density of two C1 and C5 *pseudoradical* centers (62:38) created

Preprints (www.preprints.org) | NOT PEER-REVIEWED | Posted: 27 May 2021 doi:10.20944/preprints202105.0672.v1

from the rupture of the corresponding multiple bonds along the reaction path before reaching the TS. These centres correspond with the most electrophilic carbon of iminium cation **6**, and one to the most nucleophilic centres of Cp **1**, a behaviours anticipated by analysis of the Parr functions. Interestingly, the pattern found for the C–C bond formation in this I-DA reaction is very similar to that found in N-DA and P-DA reactions [12].

Finally, an ELF comparative analysis of the TSs involved in the P-DA reactions of imines and those participating in the I-DA reactions of iminium cations, shows that there is a great similitude in the bonding changes in both polar and ionic TS. The main difference is found in the GEDT taking place in ionic reactions, higher than 0.37e; the high GEDT taking place in I-DA reactions decreases markedly the activation energies to diminish the ECs associated to the changes in electron density demanded to reach the electronic structure of the TSs.

Well established concepts in Organic Chemistry, such as electrophilicity and nucleophilicity used within MEDT permit to explain and even to predict the chemical reactivity of iminium cations participating in I-DA reactions. On the other hand, the high GEDT taking place in the cationic TSs allows explaining the low *endo* selectivity and low solvent effects found in I-DA reactions. The present MEDT study makes it possible establishing that the high GEDT taking place at the TSs of the I-DA reactions resulting of the superelectrophilic character of the iminium cations, and not steric (Pauli) repulsions such as Bickelhaup et al. have been recently proposed [29,46], are responsible for the features of these type of DA reactions.

COMPUTATIONAL DETAILS

DFT calculations were performed using the hybrid ωB97X-D functional [47], which includes long range exchange (denoted by X) correction as well as the semiclassical London-dispersion correction (indicated by suffix-D). The standard 6-311G(d,p) basis set was used [48], which includes d-type polarization for second row elements and p-type polarization functions for hydrogen atoms. The Berny method was used in optimizations [49,50]. Only one imaginary frequency characterized all studied TSs. The intrinsic reaction coordinate (IRC) paths [51] were carried out to find the unique connection given between the TSs and the minimum stationary points [52,53]. Solvent effects of acetonitrile were considered by full optimization of the gas phase structures at the same computational level using the polarizable continuum model [54,55] (PCM) in the framework of the self-consistent reaction field [56-58] (SCRF).

Preprints (www.preprints.org) | NOT PEER-REVIEWED | Posted: 27 May 2021 doi:10.20944/preprints202105.0672.v1

The GEDT [12] values were estimated by a NPA [34,35], using the equation GEDT (f) = $\sum_{q\in f} q$, were q are the atoms of a framework (f) at the TSs. CDFT reactivity indices [18,19] were calculated through the equations given in reference [19].

All calculations were carried out with the Gaussian 16 suite of programs [59]. The topology of the ELF [33] of the ωB97XD/6-311G(d,p) monodeterminantal wavefunctions was carried out using the TopMod [60] package with a cubical grid of step size of 0.1 Bohr. GaussView program [61] was used to visualize molecular geometries of all the systems as well as the position of the ELF basin attractors. The ELF localization domains at an isovalue of 0.75 a.u. were obtained with the Paraview software [62,63].

Supplementary Materials: Study of the DA reactions of imines **13** and **14** with Cp **1**. BET study of the I-DA reaction of iminium cation **6** with Cp **1**. Figure with the plot of the asynchronicity *vs* the GEDT taking place at eight of the TSs associated to the P-DA and I-DA reactions give in Scheme 1. Figure with the wB97XD/6-311G(d,p) geometries of the exo TSs of the I-DA reactions of iminium cations 6, 17-19 with Cp 1. Figure with the wB97XD/6-311G(d,p) localisation domains and ELF basin attractor positions of the *gauche 60º* **TS2** and the *anti* **TS2-*anti*** involved in the I-DA reaction of Cp **1** with iminium cation **6**, and the point of the IRC from **TS2** in which the C4–C5 distance is similar to that at the *anti* **TS2-*anti***. Table with ωB97XD/6-311G(d,p) electronic energies, in acetonitrile, of the stationary points involved in the I-DA reactions of iminium cations **6**, **15-19** with Cp **1**. Table with the ωB97XD/6-311G(d,p) thermodynamic data of the stationary points involved in the I-DA reactions of imine cation **6** with Cp **1**.

Author Contributions: L.R.D. headed the subject, wrote the manuscript, and performed calculations; M.R.-G. performed calculations and wrote the manuscript; and M.J.A. performed calculations and wrote the manuscript. All authors have read and agreed to the published version of the manuscript.

Funding: This research has received funding from the Ministry of Economy and Competitiveness (MINECO) of the Spanish Government, project PID2019-110776GB00 (AEI/FEDER, UE), and the European Union's Horizon 2020 research and innovation programme under the Marie Skłodowska-Curie grant agreement No. 84618.

Acknowledgments: The authors acknowledge the Ministry of Economy and Competitiveness (MINECO) of the Spanish Government, and the European Commission for financial support.

Conflicts of Interest: There are no conflicts to declare.

References

1. Diels, O.; Alder, K. Synthesen in der hydroaromatischen Reihe. *Justus Liebigs Ann. Chem.* 1928, **460**, 98-122.
2. Carruthers, W. *Some Modern Methods of Organic Synthesis*. second ed., Cambridge University Press: Cambridge, 1978.
3. Carruthers, W. *Cycloaddition Reactions in Organic Synthesis*; Pergamon: Oxford, 1990.
4. Woodward, R.B.; Hoffmann, R. The Conservation of the Orbital Symmetry. *Angew. Chem. Int. Ed. Engl.* **1969**, *8*, 781-853.
5. Houk, K. N.; Gonzalez, J.; Li, Y. Pericyclic Reaction Transition States: Passions and Punctilios, 1935-1995. *Acc. Chem. Res.* **1995**, *28*, 81-90.
6. X. Krokidis, S. Noury, B. Silvi, Characterization of Elementary Chemical Processes by Catastrophe Theory. *J. Phys. Chem. A* **1997**, *101*, 7277-7282.
7. Berski, S.; Andrés, J.; Silvi, B.; Domingo, L.R .The Joint Use of Catastrophe Theory and Electron Localization Function to Characterize Molecular Mechanisms. A Density Functional Study of the Diels−Alder Reaction between Ethylene and 1,3-Butadiene. *J. Phys. Chem. A* **2003**, *107*, 6014-6024.
8. Domingo, L.R.; Mar Ríos-Gutiérrez, M.; Silvi, B.; Pérez; P. The Mysticism of Pericyclic Reactions: A Contemporary Rationalisation of Organic Reactivity Based on Electron Density Analysis. *Eur. J. Org. Chem.* **2018**, 1107–1120.
9. Domingo, L.R. Molecular electron density theory: A modern view of reactivity in organic chemistry. *Molecules* **2016**, *21*, 1319.
10. K. Fukui, *Molecular Orbitals in Chemistry, Physics, and Biology*, New York, **1964**.
11. Dewar, M. J. S. Aromaticity and Pericyclic Reaction. *Angew. Chem. Int. Ed.* **1971**, *10*, 761-776.
12. Domingo, L.R. A new C-C bond formation model based on the quantum chemical topology of electron density. *RSC Adv.* **2014**, *4*, 32415–32428.
13. Domingo, L.R. Arnó, M., Andrés, J. Influence of Reactant Polarity on the Course of the Inverse-Electron-Demand Diels-Alder Reaction. A DFT Study of Regio- and

 doi:10.20944/preprints202105.0672.v1

Stereoselectivity, Presence of Lewis Acid Catalyst, and Inclusion of Solvent Effects in the Reaction between Nitroethene and Substituted Ethenes. *J. Org. Chem.* **1999**, *64*, 5867-5875.

14. Domingo, L.R.; Aurell, M.J.; Perez, P.; Contreras, R. Origin of the synchronicity on the transition structures of polar Diels-Alder reactions. Are these reactions [4+2] processes?. *J. Org. Chem.* **2003**, *68*, 3884-3890.
15. Domingo, L.R.; Sáez J.A. Understanding the mechanism of polar Diels–Alder reactions. *Org. Biomol. Chem.* **2009**, *7*, 3576-358.
16. Parr, R.G. Szentpaly, L.v.; Liu, S. Electrophilicity index. *J. Am. Chem. Soc.* **1999**, *121*, 1922–1924.
17. Domingo, L.R.; Chamorro, E.; Pérez, P. Understanding the reactivity of captodative ethylenes in polar cycloaddition reactions. A theoretical study. *J. Org. Chem.* **2008**, *73*, 4615–4624.
18. Parr, R.G.; Yang, W. *Density functional theory of atoms and molecules*, Oxford University Press, New York, 1989.
19. Domingo, L.R.; Ríos-Gutiérrez, M.; Pérez, P. Applications of the conceptual density functional indices to organic chemistry reactivity. *Molecules* **2016**, *21*, 748.
20. Terrier, F.; Sebban, M.; Goumont, R.; Hallé, J. C.; Moutiers, G.; Cangelosi, I.; Buncel, E. Dual Behavior of 4-Aza-6-nitrobenzofuroxan. A Powerful Electrophile in Hydration and σ-Complex Formation and a Potential Dienophile or Heterodiene in Diels−Alder Type Reactions. *J. Org. Chem.* **2000**, *65*, 7391–7398.
21. Domingo, L.R.; Pérez, P., The Lithium Cation Catalysed Benzene Diels-Alder reaction. Insights on the Molecular Mechanism within the Molecular Electron Density Theory. *J. Org. Chem.* **2020**, *85*, 13121−13132.
22. Mayr, H.; Ofial, A. R.; Sauer, J.; Schmied, B. [2^+ +4] Cycloadditions of Iminium Ions-Concerted or Stepwise Mechanism of Aza Diels-Alder Reactions?. *Eur. J. Org. Chem.* **2000**, 2013-2020.
23. Hedberg, C.; Pinho, P.; Roth, P.; Andersson, P. G. Diels−Alder Reaction of Heterocyclic Imine Dienophiles. J. Org. Chem. 2000, 65, 2810-2812.
24. Domingo, L.R. A Theoretical Study of the Molecular Mechanism of the Reaction between N,N-Dimethylmethyleneammonium Cation and Cyclopentadiene. *J. Org. Chem.* **2001**, *66*, 3211-3214.
25. Domingo, L.R.; Sáez, J.A.; Zaragozá, R.J.; Arnó, M. Understanding the Participation of Quadricyclane as Nucleophile in Polar [2σ + 2σ + 2π]

Cycloadditions toward Electrophilic π Molecules. *J. Org. Chem.*, **2008**, *73*, 8791-8799.

26. Domingo, L. R.; Oliva, M.; Andrés, J. A theoretical study of the reaction between cyclopentadiene and protonated imine derivatives: A shift from a concerted to a stepwise molecular mechanism. *J. Org. Chem.* **2001**, *66*, 6151-6157.
27. Domingo, L. R.; Peréz, P. A Quantum Chemical Topological Analysis of the C-C Bond Formation in Organic Reactions Involving Cationic Species. *Phys. Chem. Chem. Phys.* **2014**, *16*, 14108-14115
28. Domingo, L.R.; Perez, P.; Sáez, J. A. Understanding the local reactivity in polar organic reactions through electrophilic and nucleophilic Parr functions. *RSC Adv.* **2013**, *3*,1486-1494.
29. Vermeeren, P.; Hamlin, T.A.; Fernandez, I.; Bickelhaupt, F.M. Origin of rate enhancement and asynchronicity in iminium catalyzed Diels–Alder reactions, *Chem. Sci.* **2020**, *11*, 8105-8112.
30. Zeist, W.-J. van; Bickelhaupt, F. M. The activation strain model of chemical reactivity. *Org. Biomol. Chem.* **2010**, *8*, 3118-3127
31. Bickelhaupt, F. M. Understanding reactivity with Kohn–Sham molecular orbital theory: E2–SN2 mechanistic spectrum and other concepts *J. Comput. Chem.* **1999**, *20*, 114-128.
32. L. R. Domingo, M. J. Aurell, P. Perez, J. A. Sáez. Understanding the Origin of the Asynchronicity in Bond-Formation in Polar Cycloaddition Reactions. A DFT Study of the 1,3-Dipolar Cycloaddition Reaction of Carbonyl Ylides with 1,2-Benzoquinones. *RSC Adv.* **2012**, *2*, 1334-1342.
33. Becke, A.D. Edgecombe, K.E. A simple measure of electron localization in atomic and molecular-systems. *J. Chem. Phys.* **1990**, *92*, 5397-5403.
34. Reed, A.E.; Weinstock, R.B.; Weinhold, F. Natural population analysis. *J. Chem. Phys.*, **1985**, *83*, 735-746.
35. Reed, A.E.; Curtiss, L.A.; Weinhold, F. Intermolecular interactions from a natural bond orbital, donor-acceptor viewpoint. *Chem. Rev.*, **1988**, *88*, 899-926.
36. Pérez, P.; Domingo, L. R.; Aizman, A.; Contreras. R. The Electrophilicity Index in Organic Chemistry, In Theoretical Aspects of Chemical Reactivity. Toro-Labbe, A., Ed., Elsevier: Amsterdam, 2007, Vol. 9, pp 139−201.
37. Domingo, L.R.; Pérez, P. The Nucleophilicity N Index in Organic Chemistry. *Org. Biomol. Chem.* **2011**, *9*, 7168-7175.

38. Parr, R.G.; Pearson, R.G. Absolute hardness: Companion parameter to absolute electronegativity. *J. Am. Chem. Soc.* **1983**, *105*, 7512-7516.
39. Aurell, M. J.; Domingo, L.R.; Perez, P.; Contreras, R. A theoretical study on the regioselectivity of 1,3-dipolar cycloadditions using DFT-based reactivity indexes. *Tetrahedron*, **2004**, *60*, 11503-11509.
40. Domingo, L.R.; Aurell, M.J.; Pérez, P.; Sáez, J.A. Understanding the origin of the asynchronicity in bond-formation in polar cycloaddition reactions. A DFT study of the 1,3-dipolar cycloaddition reaction of carbonyl ylides with 1,2-benzoquinones. *RSC Adv.* **2012**, *2*, 1334-1342.
41. Hammond, G. S. A Correlation of Reaction Rates *J. Am. Chem Soc* **1955**, *77*, 334-338.
42. A Molecular Electron Density Theory Study of the Reactivity of Tetrazines in Aza-Diels-Alder Reactions. *RSC Adv.* **2020**, *10*, 15394–15405.
43. Domingo, L.R.; Ríos-Gutiérrez, M.; Pérez, P. Unveiling the Lewis Acid Catalysed Diels–Alder Reactions Through the Molecular Electron Density Theory. *Molecules* **2020**, 25, 2535.
44. Domingo, L.R.; Ríos-Gutiérrez, M.; Pérez, P. How does the global electron density transfer diminish activation energies in polar cycloaddition reactions? A Molecular Electron Density Theory study. *Tetrahedron* **2017**, *73*, 1718-1724.
45. Domingo, L.R.; Jones, R.A.; Picher, M.T.; Sepulveda-Arques, J. Theoretical study of the reaction of dimethyl acetylenedicarboxilate with 1-methyl-2-(1-substituted vinyl) pyrroles. *Tetrahedron* **1995**, *51*, 8739–8748.
46. Hamlin, T.A.; Bickelhaupt F.M., Fernández, I. The Pauli Repulsion-Lowering Concept in Catalysis. Acc. Chem. Res. 2921, 54, 1972-1981.
47. Chai, J.-D.; Head-Gordon, M. Long-range corrected hybrid density functionals with damped atom–atom dispersion corrections. *Phys. Chem. Chem. Phys.* **2008**, *10*, 6615-6620.
48. Hehre, M.J.; Radom, L.; Schleyer, P.v.R.; Pople, J. Ab initio Molecular Orbital Theory, Wiley, New York, 1986.
49. Schlegel, H.B. Optimization of equilibrium geometries and transition structures. *J. Comput. Chem.* **1982**, *3*, 214-218.
50. Schlegel, H.B. In modern electronic structure theory, Yarkony, D.R., Ed., World Scientific Publishing, Singapore, 1994.

51. Fukui, K. Formulation of the reaction coordinate. *J. Phys. Chem.* **1970**, *74*, 4161–4163
52. González, C.; Schlegel, H. B. Reaction path following in mass-weighted internal coordinates. *J. Phys. Chem.* **1990**, *94*, 5523–5527.
53. González, C.; Schlegel, H. B. Improved algorithms for reaction path following: higher-order implicit algorithms. *J. Chem. Phys.* **1991**, *95*, 5853–5860.
54. Tomasi, J.; Persico, M. Molecular interactions in solution: and overview of methods based on continuous distributions of the solvent. *Chem. Rev.*, **1994**, *94*, 2027-2094.
55. Simkin, B.Ya.; Sheikhet, I.I. Quantum chemical and statistical theory of solutions–computational approach, Ellis Horwood: London, 1995.
56. Cossi, M.; Barone, V.; Cammi, R.; Tomasi, J. Ab initio study of solvated molecules: A new implementation of the polarizable continuum model. *Chem. Phys. Lett.*, **1996**, *255*, 327-335.
57. Cances, E.; Mennucci, B.; Tomasi, J. A new integral equation formalism for the polarizable continuum model: Theoretical background and applications to isotropic and anisotropic dielectrics. *J. Chem. Phys.*, **1997**, *107*, 3032-3041.
58. Barone, V.; Cossi, M.; Tomasi, J. Geometry optimization of molecular structures in solution by the polarizable continuum model. *J. Comput. Chem.* **1998**, *19*, 404-417.
59. Gaussian 16, Revision A.03, Frisch, M.J.; Trucks, G.W.; Schlegel, H.B.; Scuseria, G.E.; Robb, M.A.; Cheeseman, J.R.; Scalmani, G.; Barone, V.; Petersson, G. A.; Nakatsuji, H.; et al. Gaussian, Inc., Wallingford CT, **2016**.
60. Noury, S.; Krokidis, X.; Fuster, F.; Silvi, B. Computational tools for the electron localization function topological analysis. *Comput. Chem.* **1999**, *23*, 597-604.
61. GaussView, Version 6.0, Dennington, R.; Keith, T.A.; Millam, J.M., Semichem Inc., Shawnee Mission, KS, **2016.**
62. Ahrens, J.; Geveci, B.; Law, C. ParaView: An End-User Tool for Large Data Visualization, Visualization Handbook, Elsevier, 2005, DOI:10.1016/B978-012387582-2/50038-1.
63. Ayachit, U. The ParaView Guide: A Parallel Visualization Application, Kitware, 2015, ISBN 978-1930934306.